

Fermi Liquid Damping and NMR Relaxation in Superconductors

S. Tewari and J. Ruvalds

*Physics Department
University of Virginia
Charlottesville, VA 22903*

(October 28, 2018)

Electron collisions for a two dimensional Fermi liquid (FL) are shown to give a quasiparticle damping with interesting frequency and temperature variations in the BCS superconducting state. The spin susceptibility which determines the structure of the damping is analyzed in the normal state for a Hubbard model with a constant on-site Coulomb repulsion. This is then generalized to the superconducting state by including coherence factors and self energy and vertex corrections. Calculations of the NMR relaxation rate reveal that the FL damping structure can reduce the Hebel-Slichter peak, in agreement with data on the organic superconductor $(MDT-TTF)_2AuI_2$. However, the strongly suppressed FL damping in the superconducting state does not eliminate the Hebel-Slichter peak, and thus suggests that other mechanisms are needed to explain the NMR data on $(TMTSF)_2ClO_4$, the BEDT organic compounds, and cuprate superconductors. Predictions of the temperature variation of the damping and the spin response are given over a wide frequency range as a guide to experimental probes of the symmetry of the superconducting pairs.

74.20.-z, 74.25.Nf, 74.70.Kn

I. INTRODUCTION

The damping of quasiparticles via electron collisions is expected to produce a T^2 variation of the resistivity in a standard Fermi liquid described by a spherical Fermi surface. In ordinary metals this contribution is so weak that it is hardly detectable [1]. However, recent discoveries of a dominant T^2 resistivity contribution in several anisotropic metals such as organic superconductors and layered cuprate and sulfide alloys provide an interesting challenge from the theoretical point of view since the observed magnitudes of such resistivities are very large. Examples [2,3] of the unconventional resistivities are shown in Figure 1.

In view of the conventional wisdom regarding the expected weakness of the electron-electron scattering contribution to the resistivity, alternate interpretations of the TiS_2 data were proposed on the basis of unusual phonon scattering. However, decisive evidence for the Fermi liquid origin of the scattering was discovered by Julien [3] in the infrared spectra of TiS_2 . These spectra show a remarkable frequency and temperature variation in accordance with the Luttinger damping for a Fermi sphere that was derived to all orders of perturbation theory for the Coulomb interaction [4]. The huge value of the resistivity of TiS_2 is on par with the data for the $Nd_{2-x}Ce_xCuO_4$ cuprate which also has a layered structure. It is also comparable to the resistivity of many organic metals such as that of $(TMTSF)_2PF_6$ shown in Figure 1. The organics have quasi-two dimensional Fermi surfaces with a high degree of anisotropy. By contrast, the much smaller resistivity of lead shown in Figure 1 provides an example of the scale set by strong electron-phonon contributions.

The purpose of the present work is to calculate the quasiparticle damping for a two dimensional electron system due to spin fluctuation scattering arising from the constant on-site Coulomb interaction U in a Hubbard model. We first compute the standard normal state damping and then focus on the influence of an isotropic superconducting energy gap on the frequency and temperature variation of the self energy. The superconducting energy gap is expected to reduce the damping in a characteristic way that depends on the symmetry of the order parameter as well as the source of the damping. The spin susceptibility, which enters in the calculation of the damping, is first analyzed for the normal electrons and then generalized to include the BCS coherence factors in the superconducting state. Our goal is to use the computed damping in a calculation of the NMR relaxation rate, with particular interest in the superconducting state response. The relaxation rate is obtained from a momentum average of the spin susceptibility that includes the calculated FL self-energy corrections. Vertex corrections to the susceptibility are also calculated and shown to be small in the regime considered in the NMR studies.

We apply our results to experimental NMR measurements on the organic superconductors. These provide insight into the structure caused by the damping as well as the symmetry of the superconducting state. The modification of the Hebel-Slichter (HS) peak is found to be particularly instructive in the case of the anomalies seen in the organics, although the general phenomenon is relevant to the high temperature cuprate superconductors as well.

Luttinger [4] originally derived the classic three dimensional Fermi liquid property of a quasiparticle damping arising from electron collisions that vanishes at the Fermi energy at zero temperature and then follows a quadratic variation in temperature T and frequency ω (measured from the Fermi energy). Hodges *et al.* [5] and others [6] calculated the quasiparticle damping and resistivity for a cylindrical Fermi surface, which introduces logarithmic corrections to the damping at low T and ω .

We first calculate the two dimensional Fermi liquid damping in the normal state by performing a momentum average over the exact spin susceptibility for a non-interacting electron gas. We then proceed to compute the susceptibility as well as the self energy in the superconducting state, and probe the influence of the calculated damping on the NMR response which involves a momentum-averaged spin susceptibility.

The original motivation for our present work was the mysterious absence of a Hebel-Slichter peak in the NMR response of high temperature cuprate superconductors [7]. The resistivity of the optimally doped cuprates above the superconducting transition is typically linear in temperature in contrast to the Fermi liquid behavior considered here. A similar physical origin of electron-electron scattering in both cases may be plausible, because alloying changes the linear T to a T^2 variation in many of the cuprates [8]. Historically the HS peak in the NMR relaxation is considered to be one of the key successes of the BCS theory since it occurs in various ordinary metals [9]. The organic superconductors yield cases where the HS peak appears, $(MDT-TTF)_2AuI_2$ [10], and also examples like $(TMTSF)_2ClO_4$ [11] where the peak is suppressed. The NMR relaxation in the BEDT [12] compounds resembles the cuprate anomalies, such as a T^3 behavior at low T in the superconducting state. Hence the present analysis is directed at the organics which often have the quadratic T variation of the resistivity that is compatible with our Fermi liquid analysis.

The absence of the coherence peak has attracted considerable previous theoretical interest. Hasegawa and Fukuyama [13] derived the NMR response for s-wave and other symmetries of the energy gap appropriate to organic superconductors. They obtained weaker, but nonetheless finite, HS peak structure for both singlet and triplet pairing states in which the order parameter exhibits line nodes on the Fermi surface. Their calculation did not include the quasiparticle damping.

Other groups have examined the effects of a strong enhancement of the quasiparticle damping near T_c , which broadens the BCS singularity in the superconducting density of states. Some theory groups have invoked a variety of phenomenological models for the damping as a function of temperature [14]. Typically, these authors use a power law variation for the T dependence of the damping (with a T^3 behavior as one example) and neglect the frequency variation. Phenomenological models have been proposed to fit the observed spin dynamics in the cuprates [15]. The “marginal” Fermi liquid response hypothesis has been used to generate a damping model which has also been applied to the NMR measurements [16].

Tight binding energy band models have also been investigated in the context of spin dynamics of cuprates by Bulut and Scalapino [17] and by Levin’s group [18]. The NMR relaxation for s and d-wave energy gaps has been calculated [14,17] using phenomenological models for the damping. The quasiparticle damping from spin fluctuations in the superconducting state has also been independently computed within a tight binding model [19].

Our analysis of the influence of the damping on the NMR spectra in the superconducting state is based on a standard approximation for the momentum-averaged spin susceptibility. This allows analytic expressions to be derived and used in the calculation of the damping, thus reducing the number of numerical integrations. However, this limits the present approach to reasonably isotropic Fermi surfaces, and cannot account for features such as nesting.

Phonon damping has furnished yet another more traditional explanation for the suppressed HS peak, provided that a large electron-phonon coupling combined with a small Coulomb pseudopotential are assumed [20]. Phonon contributions to the resistivity may be one distinguishing feature of the mechanism responsible for the NMR anomalies, and the organic resistivity data in Figure 1 provide a challenge in this regard since the T^2 variation is difficult to reconcile with phonon scattering.

Considering the wide array of theoretical proposals for the NMR anomalies, it is important to make distinctions based on specific features such as the response over a wide range of temperature, and consistency of parameters with other experimental clues. The T^2 damping which characterizes the organic superconductors considered here is one example. The temperature dependence of the NMR relaxation rate at low T is also a primary constraint on theory since it is particularly sensitive to the symmetry of the order parameter, while the HS peak structure is sensitive to the damping as well as the gap symmetry. Thus our calculations provide insight into the role of damping in the organic superconductors and the NCCO cuprate which also exhibits a T^2 resistivity above the superconducting transition.

A theoretical basis for the anomalous linear T variation of the resistivity that is an ubiquitous feature in all of the optimally doped high temperature superconductors discovered so far is the nested Fermi Liquid theory (NFL) [21]. The corresponding calculations for the NFL damping in the presence of an isotropic energy gap by Rieck *et al.* [22] reveal a very dramatic suppression of the nested spin susceptibility in the superconducting state which strongly reduces available scattering states for electron collisions. Hence the NFL damping is greatly reduced at frequencies lower than thrice the energy gap Δ . The latter damping structure is compatible with microwave surface resistance

data on the YBCO superconductor in the vicinity of T_c where the damping drops by four orders of magnitude within a few degrees of T_c . There are also numerous earlier calculations that found a sharp suppression of the damping in the case of phenomenological models that are extensions of the “marginal” Fermi liquid hypothesis [16] for the susceptibility. These are discussed in reference [22].

Recently Won and Maki [23] have shown that a nesting model yields NMR relaxation without a HS peak if indeed the scattering processes near the nesting vector form the dominant contribution to the susceptibility.

We develop the formalism for the susceptibility and self energy in section II, and present the calculated Fermi liquid damping results. The NMR relaxation is discussed in section III, and the conclusions of our study are in section IV.

II. FORMALISM

We consider the Hubbard Hamiltonian

$$H = \sum_{\mathbf{k},\sigma} \epsilon_{\mathbf{k}} c_{\mathbf{k},\sigma}^\dagger c_{\mathbf{k},\sigma} + U \sum_{\mathbf{p},\mathbf{q},\mathbf{k}} c_{\mathbf{p}+\mathbf{q},\uparrow}^\dagger c_{\mathbf{p},\uparrow} c_{\mathbf{k}-\mathbf{q},\downarrow}^\dagger c_{\mathbf{k},\downarrow}, \quad (1)$$

where $\epsilon_{\mathbf{k}}$ is the energy of an electron in two dimensions, and $c_{\mathbf{k},\sigma}^\dagger$ and $c_{\mathbf{k},\sigma}$ are the electron creation and destruction operators. The constant on-site Coulomb repulsion U restricts the scattering to spin fluctuations. Within the Born approximation considered here, the dominant effect is from the non-interacting spin susceptibility and the cross section is proportional to U^2 . In other words the self energy requires a momentum sum over $U^2\chi(\mathbf{q},\omega)$. Higher order RPA corrections will naturally enhance the cross section, but are not included here.

A. Normal State

The spin susceptibility in the normal state for non-interacting electrons is

$$\chi(\mathbf{q},\omega) = \sum_{\mathbf{k}} \frac{f(\epsilon_{\mathbf{k}+\mathbf{q}}) - f(\epsilon_{\mathbf{k}})}{\omega - \epsilon_{\mathbf{k}+\mathbf{q}} + \epsilon_{\mathbf{k}} + i\Gamma} \quad (2)$$

where $f(\epsilon)$ is the Fermi function. Within the leading order Born approximation, the imaginary part of the self energy arising from electron-electron scattering is [24]

$$\Gamma(\mathbf{k},\omega) = \frac{U^2}{2} \int d\omega' \left[\coth\left(\frac{\omega'}{2T}\right) - \tanh\left(\frac{\omega' - \omega}{2T}\right) \right] \int \frac{d\mathbf{q}}{(2\pi)^3} \chi''(\mathbf{q},\omega) \delta(\omega - \omega' - \epsilon_{\mathbf{k}+\mathbf{q}}), \quad (3)$$

where χ'' is the imaginary part of $\chi(\mathbf{q},\omega)$.

We first verified numerically that the imaginary part of the susceptibility in Eq. (2) does not vary significantly with temperature for a normal two-dimensional electron gas, and hence one may use the zero temperature analytic result in calculating Γ . Defining the frequency ω in units of $\hbar k_F^2/m$ and the wavevector q in units of the Fermi wavevector k_F , the $T = 0$ analytic form for χ'' is

$$\chi''(\mathbf{q},\omega) = \frac{N(0)}{q} \left\{ \theta \left[1 - \left(\frac{\omega}{q} - \frac{q}{2} \right)^2 \right] \left[1 - \left(\frac{\omega}{q} - \frac{q}{2} \right)^2 \right]^{\frac{1}{2}} - \theta \left[1 - \left(\frac{\omega}{q} + \frac{q}{2} \right)^2 \right] \left[1 - \left(\frac{\omega}{q} + \frac{q}{2} \right)^2 \right]^{\frac{1}{2}} \right\} \quad (4)$$

where $N(0)$ is the density of states at the Fermi level, and $\theta(x)$ is the Heaviside function that is unity for $x > 0$ and zero otherwise. Hodges [5] and others [6] have used the above analytic form to calculate the damping in the asymptotic limits of small T and ω , by performing the momentum integrations (Eq. 3) to obtain the transport lifetime. Note that the imaginary part of the self energy is $\Gamma = [1 - f(\omega)]^{-1} \hbar/\tau$ where τ is the quasiparticle transport lifetime [25].

To obtain a damping over the entire range of frequency and temperature, we employ an alternate approximation: the susceptibility in Eq. (3) is first averaged over momentum and gives at low frequencies ($\omega < \epsilon_F$),

$$\langle \chi''(\mathbf{q},\omega) \rangle_q = \frac{\pi N(0)}{W} \omega \quad (5)$$

where W is the energy bandwidth, and $N(0)$ is the density of states at the Fermi energy. We note that the momentum-averaged susceptibility is independent of temperature for the Fermi liquid. Replacing this average in Eq. (3), we

evaluate Γ numerically and find a quasiparticle damping that is quadratic in frequency and temperature. The limiting cases are

$$\Gamma(\omega = 0) = BT^2 \quad (6)$$

$$\Gamma(T = 0) = C\omega^2 \quad (7)$$

where $B = U^2 N^2(0) \pi^3 / 2W$ and $C = U^2 N^2(0) \pi / 2W$. The present method does not yield the $T^2 \ln T$ dependence found asymptotically [5,6], but the $\ln T$ correction is almost indistinguishable from T^2 at low T .

The quadratic temperature variation of our computed FL damping at two different frequencies is shown in Figure 2 for a coupling $UN(0) = 1$ and a bandwidth $W = 1$ eV. These parameters are used throughout this work. As expected, the value of the FL damping seen in Figure 2 is quite small. For comparison, the experiments that we examine suggest much larger estimates of the damping which may perhaps indicate anisotropic Fermi surface contributions, RPA enhancement of the spin susceptibility, or higher order scattering. Also, the Hubbard model restricts the Coulomb interaction to a point in real space and thus samples only the zero angular momentum scattering channel.

B. Superconducting State

In the absence of the self energy corrections from particle collisions, the BCS susceptibility in the superconducting state is modified by the presence of coherence factors due to an energy gap, and thus becomes

$$\chi(\mathbf{q}, \omega) = \sum_{\mathbf{k}} \left[A_{\mathbf{k}, \mathbf{q}}^+ \frac{f(E_{\mathbf{k}+\mathbf{q}}) - f(E_{\mathbf{k}})}{\omega - E_{\mathbf{k}+\mathbf{q}} + E_{\mathbf{k}} + i\delta} + \frac{1}{2} A_{\mathbf{k}, \mathbf{q}}^- \frac{1 - f(E_{\mathbf{k}+\mathbf{q}}) - f(E_{\mathbf{k}})}{\omega + E_{\mathbf{k}+\mathbf{q}} + E_{\mathbf{k}} + i\delta} + \frac{1}{2} A_{\mathbf{k}, \mathbf{q}}^- \frac{f(E_{\mathbf{k}+\mathbf{q}}) + f(E_{\mathbf{k}}) - 1}{\omega - E_{\mathbf{k}+\mathbf{q}} - E_{\mathbf{k}} + i\delta} \right] \quad (8)$$

where the coherence factors are

$$A_{\mathbf{k}, \mathbf{q}}^{\pm} = \frac{1}{2} \left[1 \pm \frac{\epsilon_{\mathbf{k}} \epsilon_{\mathbf{k}+\mathbf{q}} + \Delta_{\mathbf{k}} \Delta_{\mathbf{k}+\mathbf{q}}}{E_{\mathbf{k}} E_{\mathbf{k}+\mathbf{q}}} \right] \quad (9)$$

and $\Delta_{\mathbf{k}}$ is the superconducting energy gap, $\epsilon_{\mathbf{k}}$ the energy dispersion in the normal state, and $E_{\mathbf{k}} = \sqrt{\epsilon_{\mathbf{k}}^2 - \Delta_{\mathbf{k}}^2}$ the quasiparticle energy in the superconducting state. All the calculations described in this article are carried out using a superconducting gap of s-wave symmetry. The temperature dependence of the gap is taken to have the standard form that fits the solution of the BCS weak coupling gap equation,

$$\Delta(T) = \Delta_0 \tanh \left(1.76 \sqrt{\frac{T_c}{T} - 1} \right) \quad (10)$$

where $\Delta_0 = 1.76k_B T_c$. In the limit of negligible damping, $\delta \rightarrow 0^+$, the above susceptibility (Eq. 8) gives the standard sharp Hebel–Slichter peak in the NMR response.

The quasiparticle damping due to spin fluctuations in the superconducting state is [26]

$$\begin{aligned} \Gamma(\mathbf{p}, \omega) = & \frac{U^2}{[1 - f(\omega)]} \int \frac{d^2 p'}{(2\pi)^2} \left\{ \int_0^{\omega - \Delta} d\Omega \chi''(\mathbf{p} - \mathbf{p}', \Omega) \delta(\omega - \Omega - E_{\mathbf{p}'}) \left[1 + \frac{\Delta^2}{\omega(\omega - \Omega)} \right] [n(\Omega) + 1] [1 - f(\omega - \Omega)] \right. \\ & + \int_{\omega + \Delta}^{\infty} d\Omega \chi''(\mathbf{p} - \mathbf{p}', \Omega) \delta(\Omega - \omega - E_{\mathbf{p}'}) \left[1 - \frac{\Delta^2}{\omega(\Omega - \omega)} \right] [n(\Omega) + 1] f(\Omega - \omega) \\ & \left. + \int_0^{\infty} d\Omega \chi''(\mathbf{p} - \mathbf{p}', \Omega) \delta(\Omega + \omega - E_{\mathbf{p}'}) \left[1 + \frac{\Delta^2}{\omega(\Omega + \omega)} \right] n(\Omega) [1 - f(\Omega + \omega)] \right\} \end{aligned} \quad (11)$$

where $n(\omega)$ and $f(\omega)$ are the Bose and Fermi functions respectively. To simplify the multiple integrations needed for the damping, we note that the momentum variation of the susceptibility arising from a free electron dispersion is relatively smooth, in contrast to tight binding models considered, for example, by Quinlan *et al.* [19]. Hence we approximate the damping calculation by taking a momentum average of the susceptibility (for $\omega > 0$)

$$\begin{aligned} \langle \chi''(\mathbf{k}, \omega) \rangle_q = & \frac{\pi N(0)}{W} \left[2 \int_{\Delta}^{\infty} dE \frac{E(\omega + E) + \Delta^2}{\sqrt{E^2 - \Delta^2} \sqrt{(\omega + E)^2 - \Delta^2}} [f(E) - f(\omega + E)] \right. \\ & \left. + \int_{\Delta}^{\omega - \Delta} dE \frac{E(\omega - E) - \Delta^2}{\sqrt{E^2 - \Delta^2} \sqrt{(\omega - E)^2 - \Delta^2}} [1 - f(E) - f(\omega - E)] \right] \end{aligned} \quad (12)$$

The resulting calculated susceptibility average is shown in Figure 3, where the peak just below T_c at low frequencies (solid line) is a consequence of the coherence factors. At higher frequencies, as seen in the case of $\omega = 0.8\Delta_0$ (dashed line), the susceptibility drops off rapidly as T decreases though there is no coherence peak below T_c . This characteristic drop of the susceptibility below T_c is the key to determining the temperature variation of the quasiparticle damping in the superconducting state. We have used here a superconducting transition temperature $T_c = 4.2$ K, which corresponds to the organic compound $(MDT\text{-}TTF)_2\text{AuI}_2$.

We next compute the quasiparticle damping in Eq. (11) as a function of frequency and temperature for a superconductor with $T_c = 4.2$ K. The frequency dependence of Γ is shown in Figure 4 at three different temperatures, and it reveals the dramatic drop in Γ at low ω caused by the isotropic energy gap. Note that at zero temperature there is no structure in Γ below $3\Delta_0$. At higher temperatures, Γ displays an unusual frequency variation below $3\Delta(T)$, and displays a roughly quadratic increase at higher frequencies.

The temperature dependence of the computed Γ is shown in Figure 5 at three different frequencies. For frequencies below $\omega = 3\Delta_0$, the damping drops to zero at low T , but reduces to a finite value even in the zero temperature limit when the frequency exceeds thrice the energy gap.

For the calculation of the NMR relaxation rate described in the next section, we reduce the computational complexity by developing a model fit to the numerically calculated frequency and temperature dependence of the Fermi Liquid Γ at a given value of T_c . Above T_c , the damping is presumed quadratic in frequency and temperature.

III. NUCLEAR RELAXATION RATE

The standard expression for the NMR relaxation in normal metals is

$$\frac{1}{T_1 T} = |A|^2 \frac{1}{\omega_0} \sum_q \chi''(q, \omega_0) \quad (13)$$

where $|A|$ denotes the hyperfine coupling and $\omega_0 \sim 10$ MHz is the typical radio frequency of the measurement. For a Fermi Liquid, the momentum average of the spin susceptibility in Eq. (5) is linear in frequency, and thus produces the familiar Korringa relation for the nuclear relaxation that is of the form

$$\frac{1}{T_1 T} \sim |A|^2 N^2(0) = \text{constant.} \quad (14)$$

If the self energy is only weakly momentum dependent, the general form of the susceptibility in Eq. (13) can be averaged over k and q independently, and the Korringa behavior persists with very little contribution from the damping in the normal state. However, an isotropic energy gap produces a divergent density of states in the superconducting state which is naturally quite sensitive to the form of the damping. Since the above analysis demonstrates that the structure of the damping is particularly important at frequencies comparable to the energy gap, these features are important for the NMR spectra in the superconducting regime.

A. Self Energy Corrections

The NMR relaxation rate is computed using the form [27],

$$\frac{1}{T_1} = 2 |A|^2 N^2(0) \int_{\Delta}^{\infty} \frac{E dE}{\sqrt{E^2 - \Delta^2}} \int_{\Delta}^{\infty} \frac{E' dE'}{\sqrt{E'^2 - \Delta^2}} \left(1 + \frac{\Delta^2}{EE'} \right) f(E) [1 - f(E')] \frac{\Gamma}{(\omega + E - E')^2 + \Gamma^2} \quad (15)$$

where $N(0)$ is the normal state density of states at the Fermi energy, and the spin hyperfine coupling $|A|$ is taken to be constant, thereby neglecting crystalline anisotropy. The delta function in the original expression for χ'' in Eq. (13) is replaced by a Lorentzian of width Γ , the quasiparticle damping computed in Eq. (11). Thus the conventional BCS result is recovered in the limit $\Gamma \rightarrow 0$. The self energy corrections included in Eq. (15) depend on both temperature and energy, and enter as $\Gamma = \frac{1}{2} [\Gamma(E, T) + \Gamma(E', T)]$. In all the calculations discussed below, the damping is defined as

$$\Gamma = \alpha \Gamma_{\text{FL}} \quad (16)$$

where α is varied to show the consequences of enhancements beyond the Born approximation used here with one standard set of parameter values $W = 1$ eV and $UN(0) = 1$. A remarkable feature of the organic compound

resistivities shown in Figure 1 is that their high values would indicate very short mean free paths if a standard transport model is applied. However, the temperature variation of the resistance is compatible with Fermi liquid behavior, so that the enhancement remains anomalous in these cases even though the likely physical origin is electron-electron scattering. Anisotropic Fermi surface effects or higher order scattering such as the RPA corrections may be likely suspects for this mystery.

The relaxation rate data of Takahashi *et al.* [10] on the organic superconductor $(MDT-TTF)_2AuI_2$ is shown in Figure 6 along with the theoretical curves calculated using Eq. (15). The solid curve is calculated using the superconducting state quasiparticle damping computed above (Eq. 11) for the Fermi liquid. To examine the influence of the energy gap on the relaxation rate, we compare this to the dot-dashed curve calculated using the normal-state damping that is quadratic in frequency and temperature at all T and ω . Note that in both these cases the Hebel-Slichter peak is strongly reduced over the BCS result (dashed line) obtained in the absence of a broadening Γ . However, in order to fit the $(MDT-TTF)_2AuI_2$ data, the amplitude enhancement of the calculated Fermi Liquid damping needs to be $\alpha = 40$. The standard case with $\alpha = 1$ resembles the dashed BCS curve because the damping is very small.

The case of $(TMTSF)_2ClO_4$ presents an interesting challenge since the NMR data of Takigawa *et al.* [11] clearly show the absence of a Hebel-Slichter peak as seen in Figure 7. The resistivity of this organic superconductor has a temperature dependence that is close to T^2 in some samples [28], while carefully quenched samples exhibit a linear T resistivity [29]. This material is notable for nesting of the Fermi surface which gives rise to spin density wave (SDW) phase transitions in a magnetic field as discussed in terms of the nested orbit quantization by Gorkov and Lebed [30]. Our goal is to fit the NMR data using the Fermi liquid damping to see whether the damping alone can account for the suppression of the Hebel-Slichter peak. The results shown in Figure 7 reveal that the Fermi liquid damping actually gives a weak, but nevertheless significant peak in the NMR relaxation just below T_c even for very large damping cross sections. The two curves in Fig. 7 are calculated using an increase in amplitude of the damping by factors of $\alpha = 40$ and 400 respectively, and both curves are normalized to the value of $1/T_1T$ at $T_c = 1.06$ K. The $\alpha = 400$ curve resembles the data, indicating that an anomalously large damping may indeed be the cause of the suppression of the HS peak.

The data shown in Figure 8 provide another illustration of non-Fermi Liquid behavior in the organic compound $\kappa-(BEDT-TTF)_2CuN(CN)_2Br$. The NMR relaxation rate data of Kanoda *et al.* [12] on this organic compound are shown (dots) along with the theoretical curve (solid line) calculated using the Fermi Liquid damping and enhancement $\alpha = 40$. Unlike the calculated curve, the data show no evidence of a Hebel-Slichter peak, and also drop much more sharply at low temperatures than the calculated curves. The conventional BCS result with a more pronounced coherence peak is also shown (dashed line). The data for this organic compound exhibit a T^3 temperature dependence at low T , which is suggestive of an unconventional pairing state with line nodes on the Fermi surface, *e.g.* d-wave pairing. In the normal state the data are also anomalous in that they do not follow a Korringa law [31]. A peak in $1/T_1$ is observed at 50 K which tends to vanish under pressure [32]. This pressure variation of T_1T in the normal state may arise from spin fluctuations whose contributions increase with the degree of nesting of the Fermi surface.

B. Vertex Corrections

The NMR relaxation rate discussed above has been calculated in the presence of self energy corrections to the spin susceptibility. Schrieffer [33] has raised the issue of the importance of vertex corrections for pairing schemes that rely on the exchange of spin fluctuations, suggesting that the pairing coupling may be strongly suppressed. We have addressed this question in the case of the lowest order bubble susceptibility $\chi(q, \omega)$. We are interested in vertex corrections to the NMR relaxation rate consistent with the Ward identity. Since $1/T_1T = \lim_{\omega \rightarrow 0} \sum_q \chi''(q, \omega)/\omega$, it suffices to calculate the correction to the momentum averaged imaginary part of the spin susceptibility. Wermbter and Tewordt [34] have used strong coupling Eliashberg theory to compute the vertex corrections within a 2D Hubbard model for an interaction arising from the exchange of spin and charge fluctuations as well as phonons. In their calculations, they approximate the bubble susceptibility $\chi(q, \omega)$ by its average over momentum. Their approach is thus a good starting point for our calculation which is carried out in the weak coupling limit for the lowest order electron-hole bubble.

In the absence of self-energy and vertex corrections, the momentum average of the imaginary part of the susceptibility is given by the expression for $1/T_1T$ in Eq. (15). Including vertex corrections to order U^2 , the one-loop contribution relevant to the spin fluctuations becomes [34]

$$\bar{\chi}''(\omega) = \pi \int_{-\infty}^{\infty} dE \frac{E(E + \omega) + \Delta^2}{\sqrt{E^2 - \Delta^2} \sqrt{(E + \omega)^2 - \Delta^2}} [f(E)[1 - J_1(E, \omega) + \pi^2 J_2(E, \omega)] - f(E + \omega)[1 - J_1(E, \omega) + \pi^2 J_2'(E, \omega)]] \quad (17)$$

where $\bar{\chi}'' = \langle \chi''(\mathbf{q}, \omega) \rangle_q$ is the momentum-averaged susceptibility. The correction terms J_1, J_2 are given by

$$J_1(E, \omega) = -\frac{U^2 N^2(0)}{2\pi} \int_{-\infty}^{\infty} d\nu \bar{\chi}''(\nu) \int_{-\infty}^{\infty} d\mu_1 \frac{f(-\mu_1) + n(\nu)}{\sqrt{\mu_1^2 - \Delta^2}} \int_{-\infty}^{\infty} \frac{d\mu_2}{\omega - \mu_2} \left\{ \frac{|\mu_1| |\mu_1 - \mu_2| + \Delta^2}{(E + \omega - \mu_1 - \nu) \sqrt{(\mu_1 - \mu_2)^2 - \Delta^2}} - \frac{|\mu_1| |\mu_1 + \mu_2| + \Delta^2}{(E - \mu_1 - \nu) \sqrt{(\mu_1 + \mu_2)^2 - \Delta^2}} \right\} \quad (18)$$

where $f(x), n(x)$ are the Fermi and Bose functions respectively, and

$$J_2(E, \omega) = -\frac{U^2 N^2(0)}{2\pi} \int_{-\infty}^{\infty} d\nu \bar{\chi}''(\nu) [f(\nu - E - \omega) + n(\nu)] \frac{|E + \omega - \nu| |E - \nu| + \Delta^2}{\sqrt{(E + \omega - \nu)^2 - \Delta^2} \sqrt{(E - \nu)^2 - \Delta^2}}. \quad (19)$$

The term J'_2 in Eq. (17) is obtained from J_2 by substituting $f(\nu - E)$ for $f(\nu - E - \omega)$.

The NMR relaxation rate is obtained from the $\omega \rightarrow 0$ limit of $\bar{\chi}''(\omega)$ in Eq. (17). We therefore calculate $J_1(E, 0)$ and $J_2(E, 0)$, noting that $J'_2(E, 0) \equiv J_2(E, 0)$. The μ_2 integration in Eq. (18) can be carried out analytically, giving

$$J_1(E, 0) = \frac{U^2 N^2(0)}{\pi} \int_{-\infty}^{\infty} d\nu \bar{\chi}''(\nu) \int_{-\infty}^{\infty} d\mu_1 [\coth \frac{\nu}{2T} + \tanh \frac{\mu_1}{2T}] \frac{1}{(E - \mu_1 - \nu)} \frac{\Delta^2}{(\mu_1^2 - \Delta^2)} \ln \left| \frac{\mu_1 + \sqrt{\mu_1^2 - \Delta^2}}{\mu_1 - \sqrt{\mu_1^2 - \Delta^2}} \right|. \quad (20)$$

In the low temperature limit, $T \rightarrow 0$, we can obtain an estimate of the vertex contribution by replacing $\coth(x/2T)$, and $\tanh(x/2T)$ by $\text{sgn}(x)$, and the μ_1 integration in Eq. (20) can also be carried out analytically. The remaining ν integrations in J_1 and J_2 (Eq. 19) are carried out numerically. In the limit $\omega \rightarrow 0$, Eq. (17) becomes

$$\frac{1}{T_1 T} \propto \lim_{\omega \rightarrow 0} \frac{1}{\omega} \bar{\chi}''(\omega) = \pi \int_{-\infty}^{\infty} dE \frac{E^2 + \Delta^2}{E^2 - \Delta^2} \left(-\frac{\partial f}{\partial E} \right) [1 - J_1(E, 0) + \pi^2 J_2(E, 0)] \quad (21)$$

The resulting total vertex correction, $-J_1(E, 0) + \pi^2 J_2(E, 0)$ is shown in Figure 9. We find that the contribution of J_1 is approximately an order of magnitude larger than J_2 for $T < T_c$. Since J_1 is proportional to Δ^2 , the correction is larger for a system with higher T_c . This is illustrated in Figure 9 for $T_c = 10, 20, 100$ K. We find that J_1 decreases with increasing temperature, and vanishes as $T \rightarrow T_c$ since $\Delta \rightarrow 0$. In this limit, $J_2(E, 0) \rightarrow -U^2 N^2(0) [\pi^2 T^2 + E^2] / 4W^2$, which is small for $E \ll W$. The temperature dependence of J_2 reveals that $J_2(T < T_c) < J_2(T_c)$ for all E . Thus the total correction term decreases as T increases. The transition temperatures of the organics are at most of the order of 10 K, and the total vertex correction for $T_c = 10$ K is less than 3%. We also find from Figure 9 that at a fixed temperature, regardless of the value of T_c , the correction does not depend strongly on E . It can thus be taken out of the integral in Eq. (21) and the net result is a renormalized value of the interaction strength U .

We basically concur with the conclusions of Wermbter and Tewordt [34] who estimated vertex contributions by another method and found them to be negligible for their choice of parameters.

IV. CONCLUSIONS

We have calculated the quasiparticle damping Γ arising from electron-electron collisions in a two dimensional Fermi Liquid. We have presented results for the temperature and frequency variation of Γ in the normal and the superconducting state with an isotropic energy gap. The damping is found to be quadratic in temperature and frequency above the superconducting transition, consistent with the T^2 resistivity of the organic superconductors and the $\text{Nd}_{2-x}\text{Ce}_x\text{CuO}_4$ cuprate.

The computed damping follows an unusual frequency variation in the superconducting state for frequencies $\omega < 3\Delta(T)$. The reduction in available scattering states due to the opening of an isotropic energy gap causes the quasiparticle damping to drop at temperatures below the superconducting transition, as seen in our results. On the other hand an energy gap of d-wave symmetry has nodes and thus ensures the availability of scattering states even at $T = 0$. This would produce a quasiparticle damping that drops less rapidly as T decreases below T_c .

We have also explored the influence of the calculated FL damping on the NMR relaxation rate. We find that the damping acts to reduce the magnitude of the Hebel-Slichter peak below T_c , but does not eliminate it. Our results are compared to experimental data on three organic superconductors. In the case of $(\text{MDT-TTF})_2\text{AuI}_2$, our results fit the data and reproduce the weak HS peak seen in the experiment. In the case of $(\text{TMTSF})_2\text{ClO}_4$, the data show no HS peak and deviate from our FL results. We find, however, that if the damping is made anomalously large, our

results resemble the data on $(\text{TMTSF})_2\text{ClO}_4$, though a small HS peak is still present in the calculations. Since the HS peak is sensitive to the BCS coherence factors, the gap symmetry and the quasiparticle damping, the analogous “coherence peak” in the microwave conductivity should provide a further test of our analysis. Applications of the FL damping to microwave conductivity and surface resistance measurements on the NCCO cuprate [35] reveal that these probes are also sensitive to the self-energy structure [36].

The NMR data on the BEDT organic superconductors exhibit a very rapid decrease below T_c that is similar to the behavior seen in the high temperature cuprate superconductors. These cases appear to require additional mechanisms to explain the lack of a Hebel-Slichter peak as well as the curvature of the NMR relaxation below T_c . Our microscopic analysis yields a relaxation curve that remains considerably higher than the BEDT data in the superconducting state even if the Coulomb coupling is artificially increased to unrealistic values.

The influence of the symmetry of the gap on the relaxation rate may be seen from the behavior of the density of states. For an s-wave gap, the superconducting density of states is zero below Δ and has a square root singularity at Δ . The density of states for a d-wave gap is linear at low energies and has only a logarithmic singularity at Δ . While the Hebel Slichter peak is greatly reduced as a result of replacing a square root singularity by a logarithmic one, the relaxation rate in the d-wave case falls off more slowly than the s-wave case as T decreases below T_c . At low temperatures, the d-wave relaxation rate varies as T^3 , and the BEDT data provide evidence for the latter symmetry.

We note here that in the case of the NFL damping calculated for a nested Fermi surface by Rieck *et al.* [22], the quasiparticle damping drops to zero at frequencies $\omega < 3\Delta$ more rapidly than the FL damping discussed here. Also the nesting generates an enhanced peak in the susceptibility at the nesting vector whose suppression by an isotropic energy gap is more pronounced than the case of the averaged susceptibility that dominates the Fermi liquid response in the present work.

The extension of the present analysis to incorporate a d-wave energy gap is in progress. Future studies of a model Fermi surface that includes nesting features are warranted in view of the remaining anomalies in the NMR spectra of the BEDT organic compound as well as the cuprate superconductors.

ACKNOWLEDGMENTS

It is a pleasure to thank Attila Virosztek for helpful discussions, and David Djajaputra, Carsten Rieck and Jeff Thoma for their input. We thank K. Kanoda for sending us their preprint and T. Takahashi for useful exchanges. We also thank K. Kanoda, T. Takahashi and M. Takigawa for use of their data. This work was supported by DOE Grant No. DEFG05-84ER45113.

-
- [1] N. W. Ashcroft and N. D. Mermin, *Solid State Physics* (Holt, Rinehart and Winston, New York, 1975).
 - [2] See review by L. N. Bulaevskii, *Adv. Phys.* **37**, 443 (1988); $(\text{TMTSF})_2\text{PF}_6$ data from K. Bechgaard *et al.*, *Sol. St. Comm.* **33**, 1119 (1980); NCCO data from Y. Hidaka and M. Suzuki, *Nature* **338**, 635 (1989); Pb data from J. P. Moore and R. S. Graves, *J. Appl. Phys.* **44**, 1174 (1973).
 - [3] C. Julien, J. Ruvalds, A. Virosztek and O. Gorochov, *Sol. St. Comm.* **79**, 875 (1991).
 - [4] J. M. Luttinger, *Phys. Rev.* **121**, 942 (1961).
 - [5] C. Hodges, H. Smith and J. W. Wilkins, *Phys. Rev. B* **4**, 302 (1971). See also A. V. Chaplik, *Zh. Teor. Fiz.* **60**, 1845 (1971) [*Sov. Phys. JETP* **33**, 997 (1971)].
 - [6] G. F. Giuliani and J. J. Quinn, *Phys. Rev. B* **26**, 4421 (1982).
 - [7] See, for example, the reviews by R. E. Walstedt and W. W. Warren, *Science* **248**, 1082 (1990); C. H. Pennington and C. P. Slichter in *Physical Properties of High Temperature Superconductors II*, edited by D. M. Ginsberg (World Scientific, Singapore, 1990).
 - [8] H. Takagi *et al.*, *Phys. Rev. Lett.* **69**, 2975 (1992).
 - [9] L. C. Hebel and C. P. Slichter, *Phys. Rev.* **113**, 1504 (1959); see also review by D. E. MacLaughlin, *Solid State Physics* **31**, edited by H. Ehrenreich, F. Seitz and D. Turnbull (Academic Press, New York, 1976).
 - [10] T. Takahashi *et al.*, *Physica C* **235-240**, 2461 (1994).
 - [11] M. Takigawa, H. Yasuoka and G. Saito, *J. Phys. Soc. Jpn.* **56**, 873 (1987).
 - [12] K. Kanoda, K. Miyagawa, A. Kawamoto and Y. Nakazawa, *preprint*.
 - [13] Y. Hasegawa and H. Fukuyama, *J. Phys. Soc. Jpn.* **56**, 877 (1987).
 - [14] L. Coffey, *Phys. Rev. Lett.* **64**, 1071 (1990); Q. P. Li and R. Joynt, *Phys. Rev. B* **47**, 530 (1993); A. Sudbø *et al.*, *Phys. Rev. B* **49**, 12245 (1994).

- [15] H. Monien and D. Pines, Phys. Rev. B **41**, 6297 (1990); A. J. Millis, H. Monien and D. Pines, Phys. Rev. B **42**, 167 (1990).
- [16] C. M. Varma *et al.*, Phys. Rev. Lett. **63**, 1996 (1989); Y. Kuroda and C. M. Varma, Phys. Rev. B **42**, 8619 (1990); M. Nuss *et al.*, Phys. Rev. Lett. **66**, 3305 (1991); P. B. Littlewood and C. M. Varma, J. Appl. Phys. **69**, 4979 (1991); Phys. Rev. B **46**, 405 (1992).
- [17] N. Bulut *et al.*, Phys. Rev. B **41**, 1797 (1990); N. Bulut and D. J. Scalapino, Phys. Rev. Lett. **68**, 706 (1992) and Phys. Rev. B **45**, 2371 (1992).
- [18] J. P. Lu, Q. Si, J. H. Kim and K. Levin, Phys. Rev. Lett. **65**, 2466 (1990).
- [19] S. M. Quinlan, D. J. Scalapino and N. Bulut, Phys. Rev. B **49**, 1470 (1994).
- [20] P. B. Allen and D. Rainer, Nature **349**, 396 (1991); A. V. Dolgov, A. A. Golubov and A. E. Koshelev, Solid St. Comm. **72**, 81 (1989); R. Akis and J. P. Carbotte, Sol. St. Comm. **78**, 393 (1991).
- [21] A. Virosztek and J. Ruvalds, Phys. Rev. B **42**, 4064 (1990).
- [22] C. T. Rieck *et al.*, Phys. Rev. B **51**, 3772 (1995).
- [23] H. Won and K. Maki, Physica B **206**, 664 (1995).
- [24] A. A. Abrikosov, L. P. Gorkov, and I. E. Dzyaloshinski, *Methods of Quantum Field Theory in Statistical Physics* (Prentice-Hall, New Jersey, 1963).
- [25] G. D. Mahan, *Many-Particle Physics* (Plenum, New York, 1990).
- [26] L. Tewordt, Phys. Rev. **127**, 371 (1962); **128**, 12 (1962); S. B. Kaplan *et al.*, Phys. Rev. B **14**, 4854 (1976).
- [27] J. R. Schrieffer, *Theory of Superconductivity* (Benjamin, New York, 1964).
- [28] K. Bechgaard *et al.*, Phys. Rev. Lett. **46**, 852 (1981).
- [29] H. Schwenk, K. Andres and F. Wudl, Phys. Rev. B **29**, 500 (1984).
- [30] L. P. Gorkov and A. G. Lebed, J. Physique Lett. **45**, L533 (1984).
- [31] A. Kawamoto *et al.*, Phys. Rev. Lett. **74**, 3455 (1995).
- [32] H. Mayaffre *et al.*, Europhys. Lett. **28**, 205 (1994).
- [33] J. R. Schrieffer, J. Low Temp. Phys. **99**, 397 (1995).
- [34] S. Wermbter and L. Tewordt, Phys. Rev. B **44**, 9524 (1991); Physica C **199**, 375 (1992).
- [35] S. M. Anlage *et al.*, Phys. Rev. B **50**, 523 (1994).
- [36] S. Tewari and J. Ruvalds, *in preparation*.

FIG. 1. The resistivity as a function of temperature is shown for various materials at temperatures above the superconducting transition. Note that the resistivity of Pb at these temperatures is linear in T (above the Debye temperature) and is much lower than that of the organic metal $(\text{TMTSF})_2\text{PF}_6$ and the layered compounds TiS_2 and $\text{Nd}_{1.84}\text{Ce}_{0.16}\text{CuO}_{4-y}$, whose resistivities show a quadratic dependence on temperature. This T^2 variation resembles Fermi Liquid damping with an anomalous enhancement of the electron-electron scattering.

FIG. 2. The normal state quasiparticle damping $\Gamma(\omega)$ (*i.e.* the imaginary part of the self energy) for a two dimensional Fermi liquid is plotted as a function of temperature at two different frequencies, $\omega = 0.01$ eV and $\omega = 10^{-4}$ eV. The standard values of the coupling $UN(0) = 1$ and bandwidth $W = 1$ eV produce the small magnitude of Γ .

FIG. 3. The momentum averaged BCS susceptibility in the superconducting state is plotted as a function of temperature at two frequencies, $\omega = 0.1\Delta_0$ and $\omega = 0.8\Delta_0$, for a transition temperature $T_c = 4.2$ K. Note that the overall decrease in $\langle\chi''\rangle_q$ at very low T remains a feature at all frequencies, while the coherence peak is only visible at lower frequencies.

FIG. 4. The calculated quasiparticle damping in the superconducting state is plotted as a function of frequency at three different temperatures. We have used here the parameters $UN(0) = 1$, $W = 1$ eV and $T_c = 4.2$ K. Note that at $T = 0$ the damping vanishes below $\omega = 3\Delta_0$. At higher temperatures, however, there is a finite response below $3\Delta(T)$ with an unusual frequency variation. The damping is quadratic in frequency for $\omega > 3\Delta(T)$.

FIG. 5. The calculated quasiparticle damping in the superconducting state is plotted as a function of temperature at three different frequencies. We use the transition temperature $T_c = 4.2$ K, and $UN(0) = 1$, $W = 1$ eV. In the normal state, the damping is quadratic in temperature. As T decreases below the superconducting transition, the damping drops rapidly to zero at low frequencies (*i.e.* $\omega \leq 3\Delta_0$) and saturates at a value that depends on the frequency at higher ω .

FIG. 6. The NMR relaxation rate $1/T_1T$ data of Takahashi *et al.* on the organic superconductor $(MDT-TTF)_2AuI_2$ are plotted as a function of temperature at a frequency $\omega = 42$ MHz. The data show a weak Hebel-Slichter peak below $T_c = 4.2K$. Also shown are the theoretical curves for $1/T_1T$ using the calculated Fermi liquid quasiparticle damping Γ_{FL} that includes the energy gap (solid line), and a normal state damping that is quadratic in frequency and temperature at all T and ω (dot-dashed line). The dashed line represents the conventional BCS result in the limit $\Gamma \rightarrow 0$. In order to fit the $(MDT-TTF)_2AuI_2$ data, the amplitude of the Fermi Liquid damping Γ_{FL} is increased by a factor of $\alpha = 40$. The calculated curves as well as the data have been normalized to the value of $1/T_1T$ at T_c .

FIG. 7. The NMR relaxation rate $1/T_1T$ data of Takigawa *et al.* on the organic superconductor $(TMTSF)_2ClO_4$ is shown (dots) as a function of temperature at a frequency $\omega = 42$ MHz. This material has a transition temperature $T_c = 1.06K$ and does not display a Hebel-Slichter peak below T_c . Also shown are the theoretical curves for $1/T_1T$ using the calculated Fermi liquid quasiparticle damping Γ_{FL} where the magnitude of the damping is increased over the calculated value by a factor α . The curves are shown for two different values of α . The theoretical curves have been normalized to the value of the $1/T_1T$ data at $T = T_c$. Note that even when α is made unrealistically large, the coherence peak is present in the calculations.

FIG. 8. The NMR relaxation rate $1/T_1T$ data of Kanoda *et al.* on the organic superconductor $\kappa-(BEDT-TTF)_2CuN(CN)_2Br$ is plotted as a function of temperature at a frequency $\omega = 25$ MHz. The solid line represents the theoretical curve for $1/T_1T$ using the calculated Fermi liquid quasiparticle damping $\alpha\Gamma_{FL}$ where the magnitude of the damping is increased over the bare value by a factor $\alpha = 40$. Also shown is the BCS result (dashed line) for which the coherence peak is more pronounced. The theoretical curves as well as the data have been normalized to the value of $1/T_1T$ at $T_c = 12$ K. The low temperature T^3 variation of the data resembles d-wave pairing behavior, and the pressure variation of the normal state T_1T may indicate spin fluctuation contributions which are enhanced by Fermi surface nesting, that is beyond the scope of the present analysis.

FIG. 9. The total contribution $J(E)$ from the calculated vertex corrections to the NMR relaxation rate is plotted as a function of the energy E scaled to the energy gap Δ at a fixed temperature $T = 1K$. The three curves correspond to superconducting transition temperatures of $T_c = 100, 20$ and 10 K. The correction increases with T_c as seen in the figure. For a fixed T_c the vertex contribution at the $T = 1$ K value chosen here is close to the maximum and falls off as the temperature approaches T_c . For $T_c = 10$ K, the magnitude of the correction at $E = 4\Delta$ is $< 3\%$, and thus negligible. We also note that since $J(E)$ is practically independent of E , the effect of this correction is to renormalize the interaction strength U .

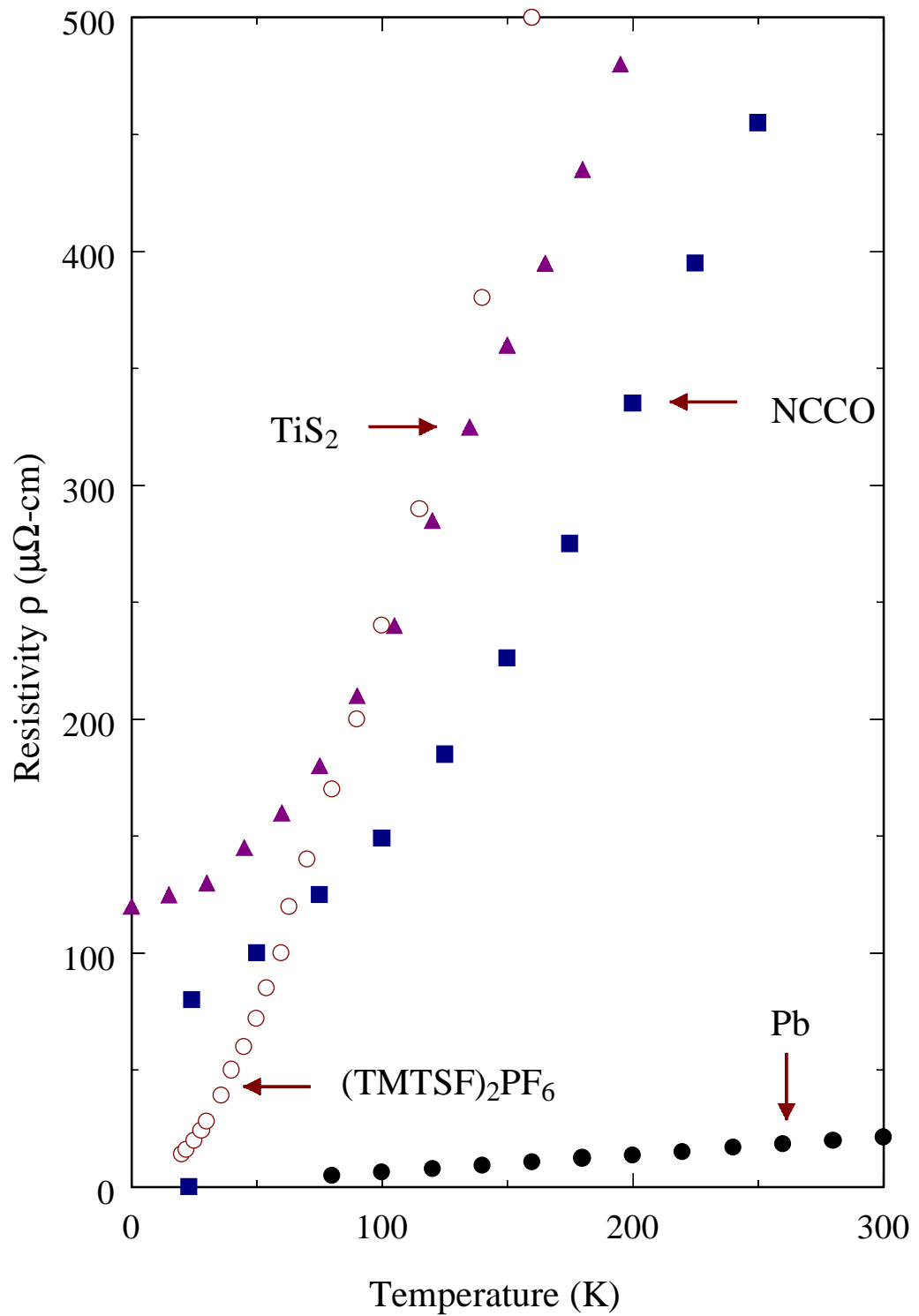


FIGURE 1

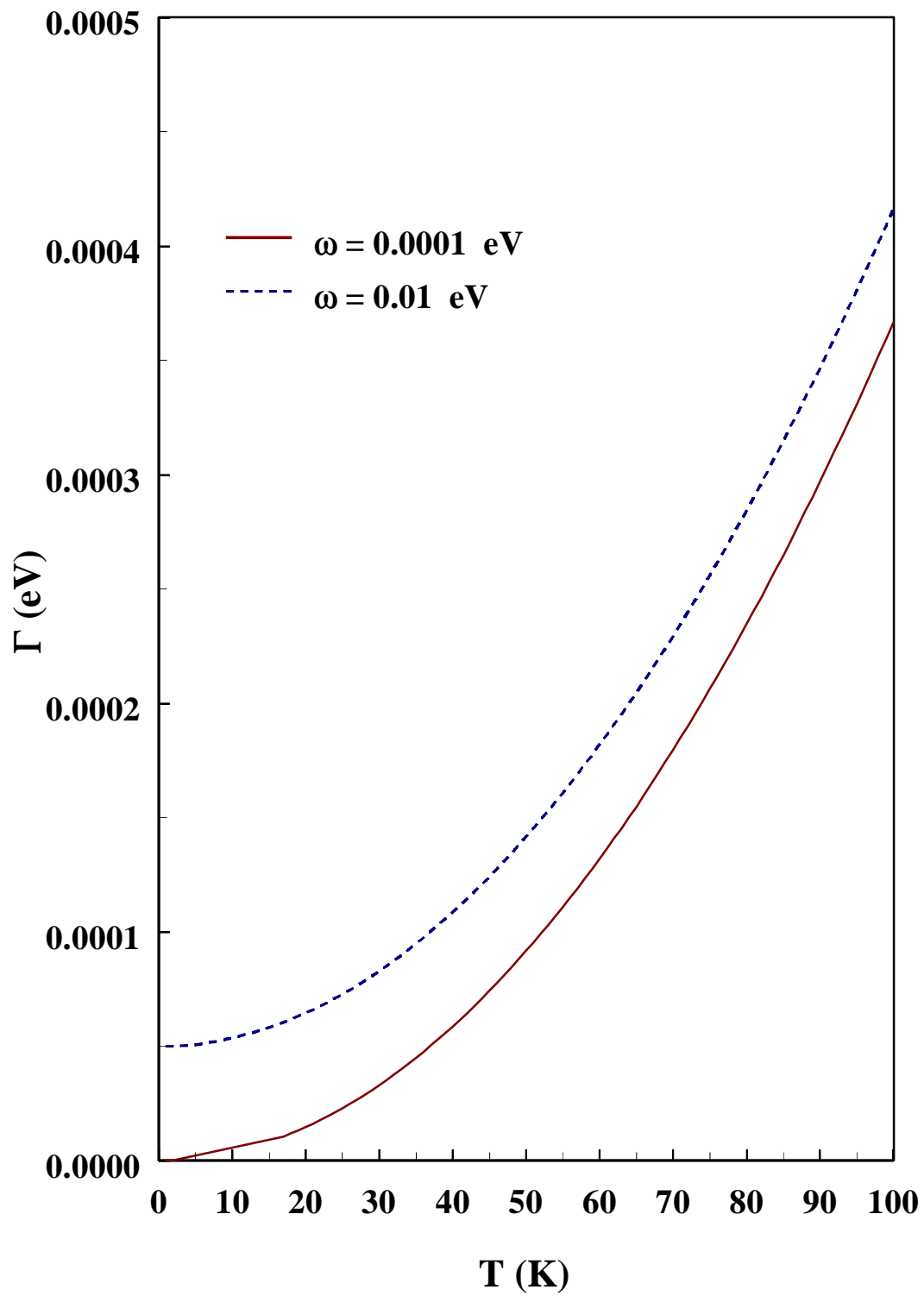


FIGURE 2

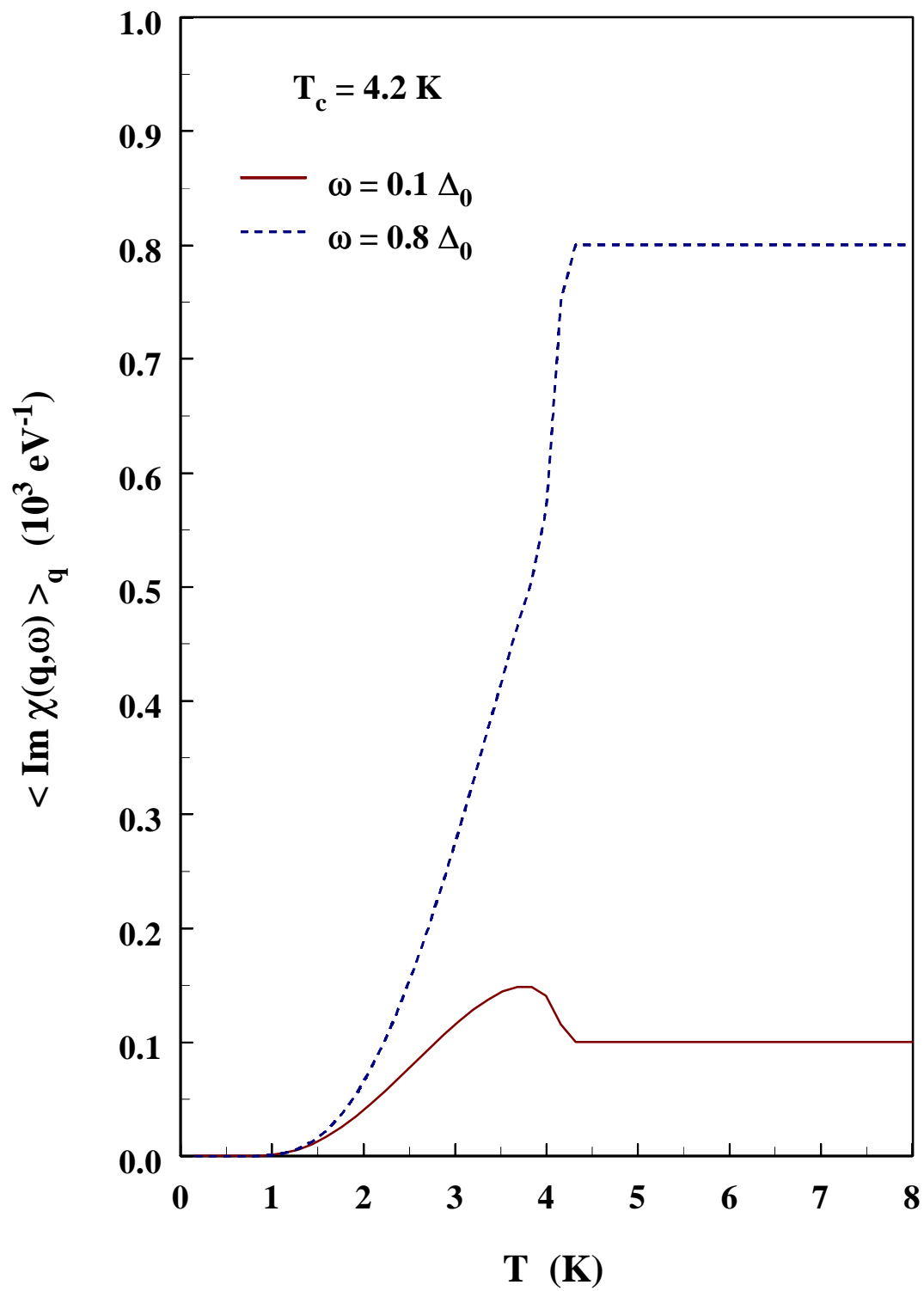


FIGURE 3

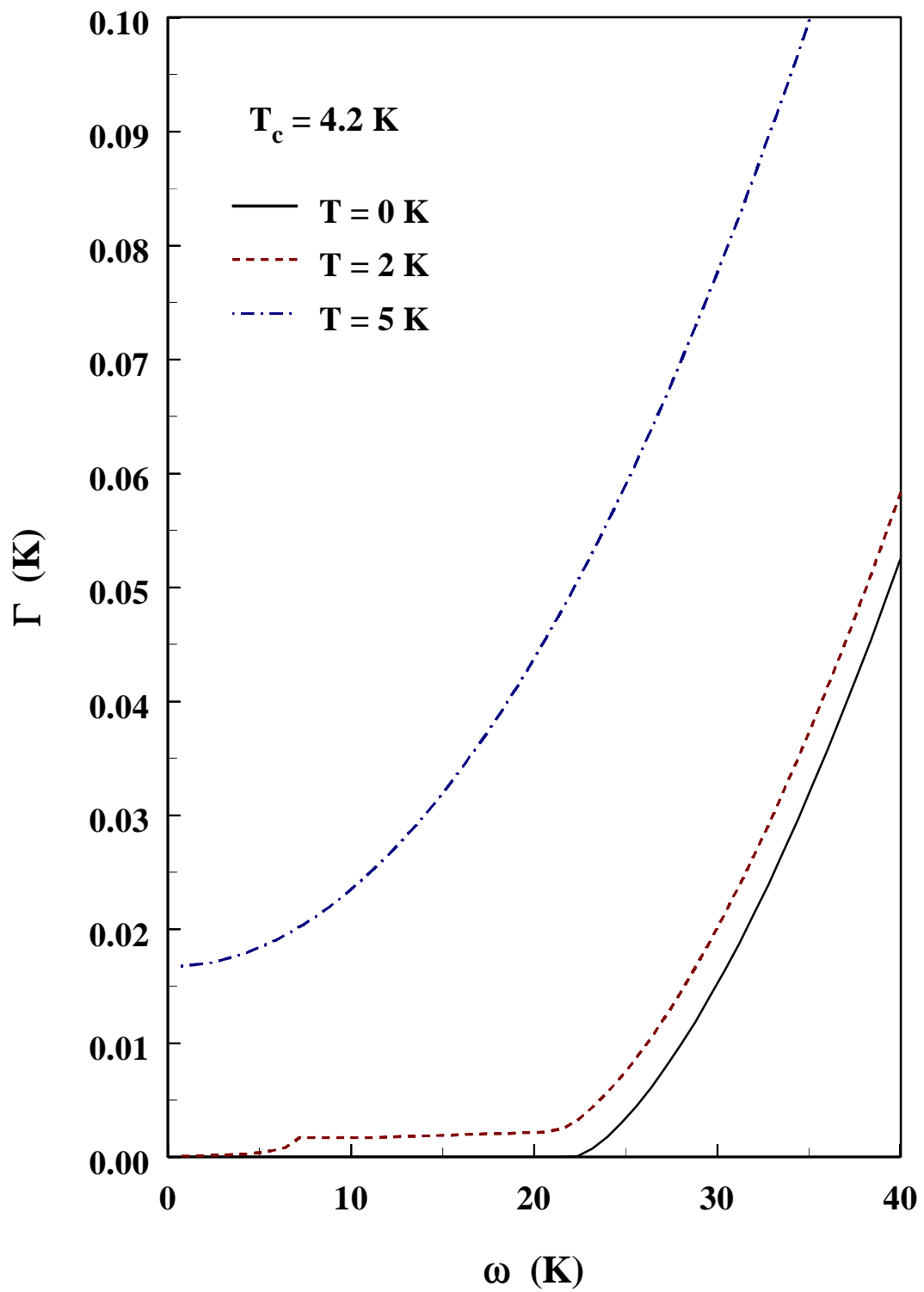


FIGURE 4

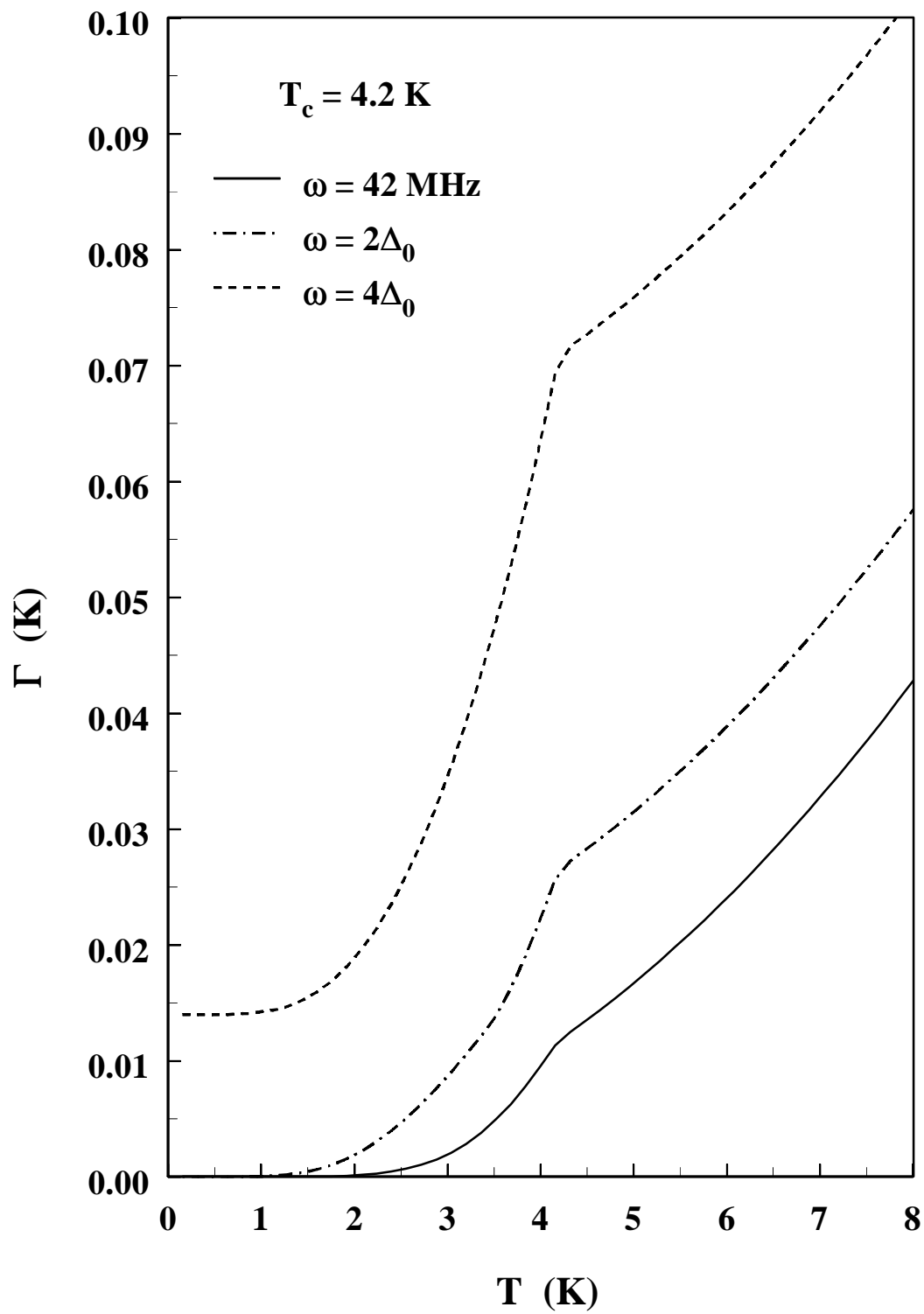


FIGURE 5

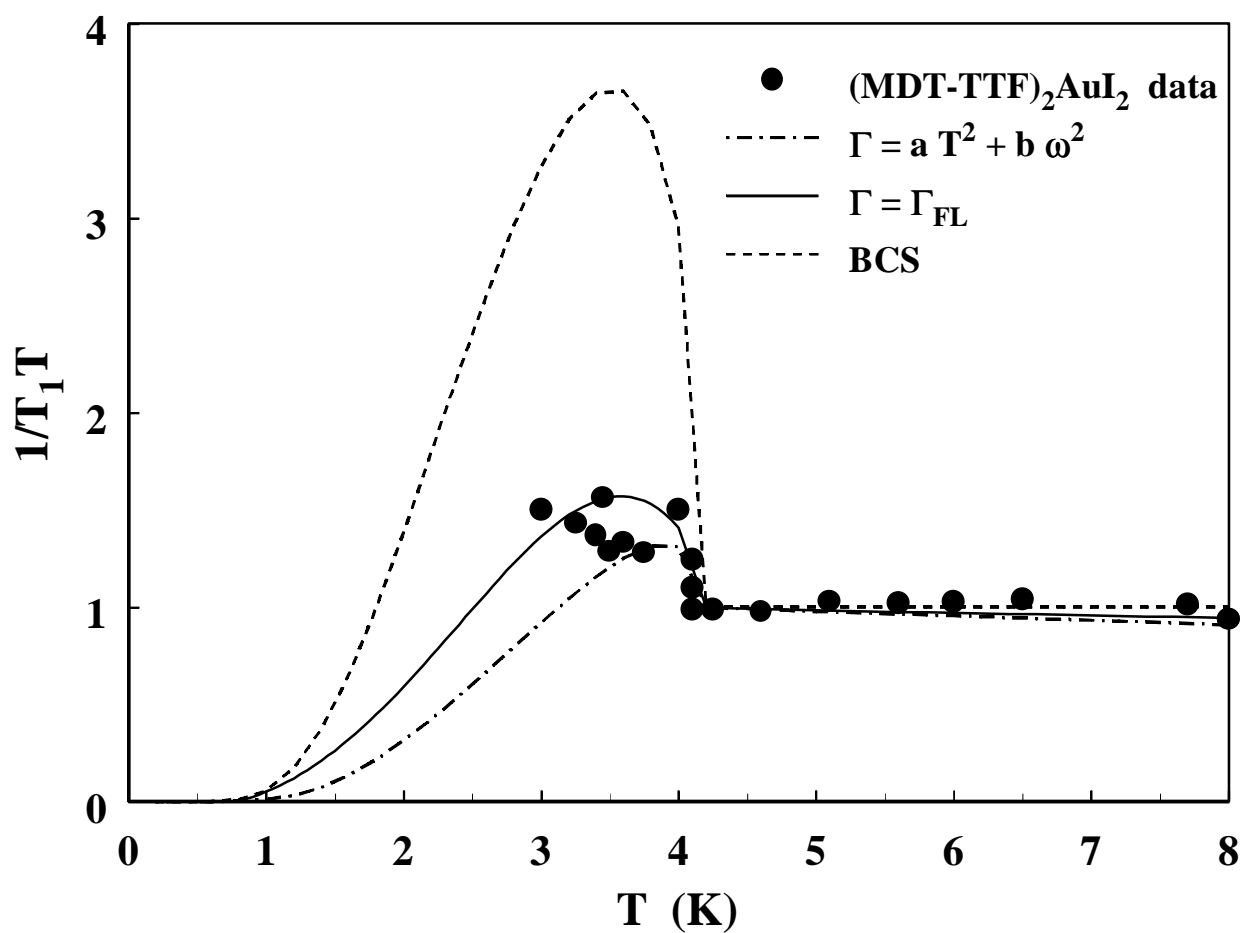


FIGURE 6

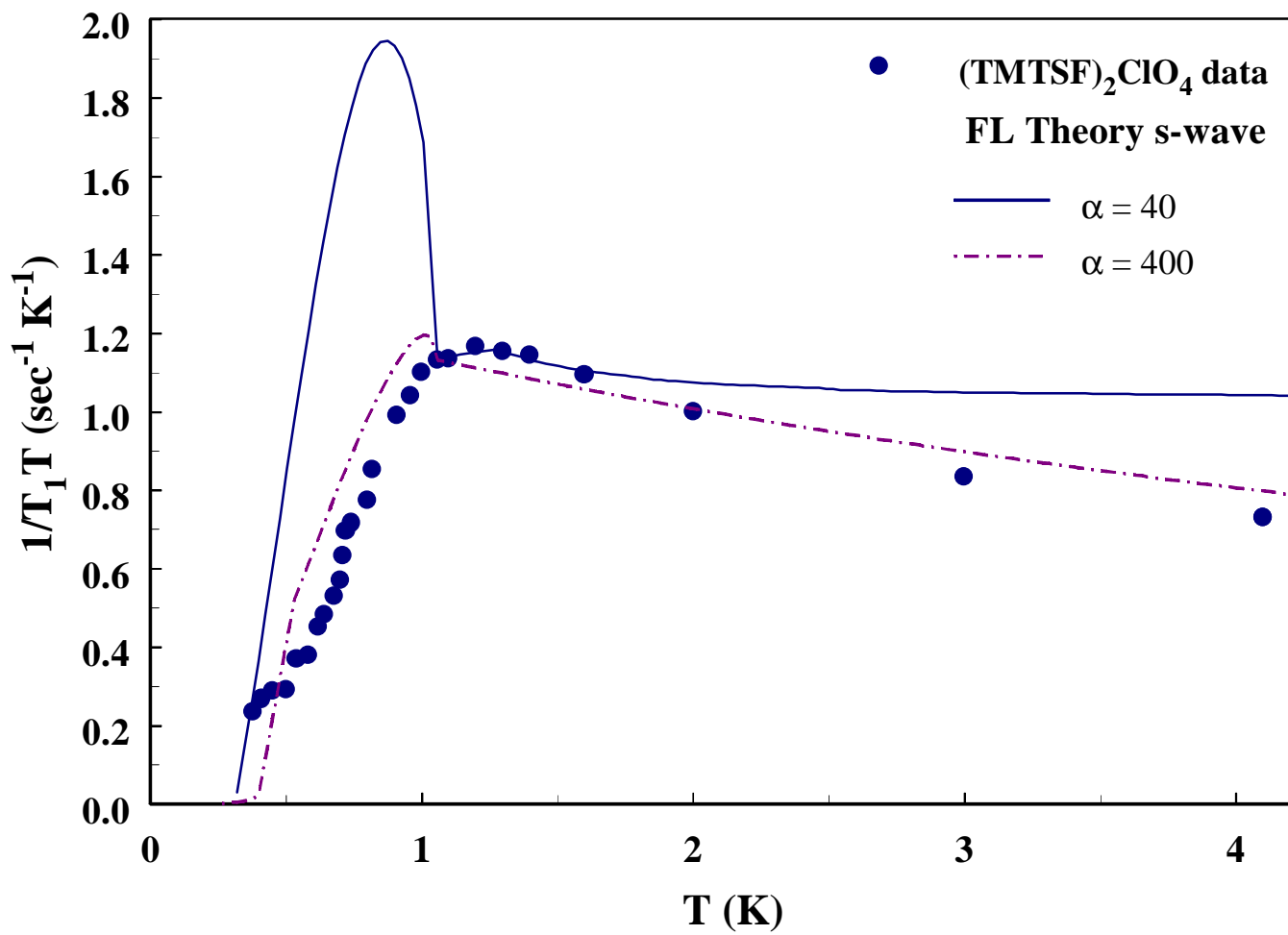


FIGURE 7

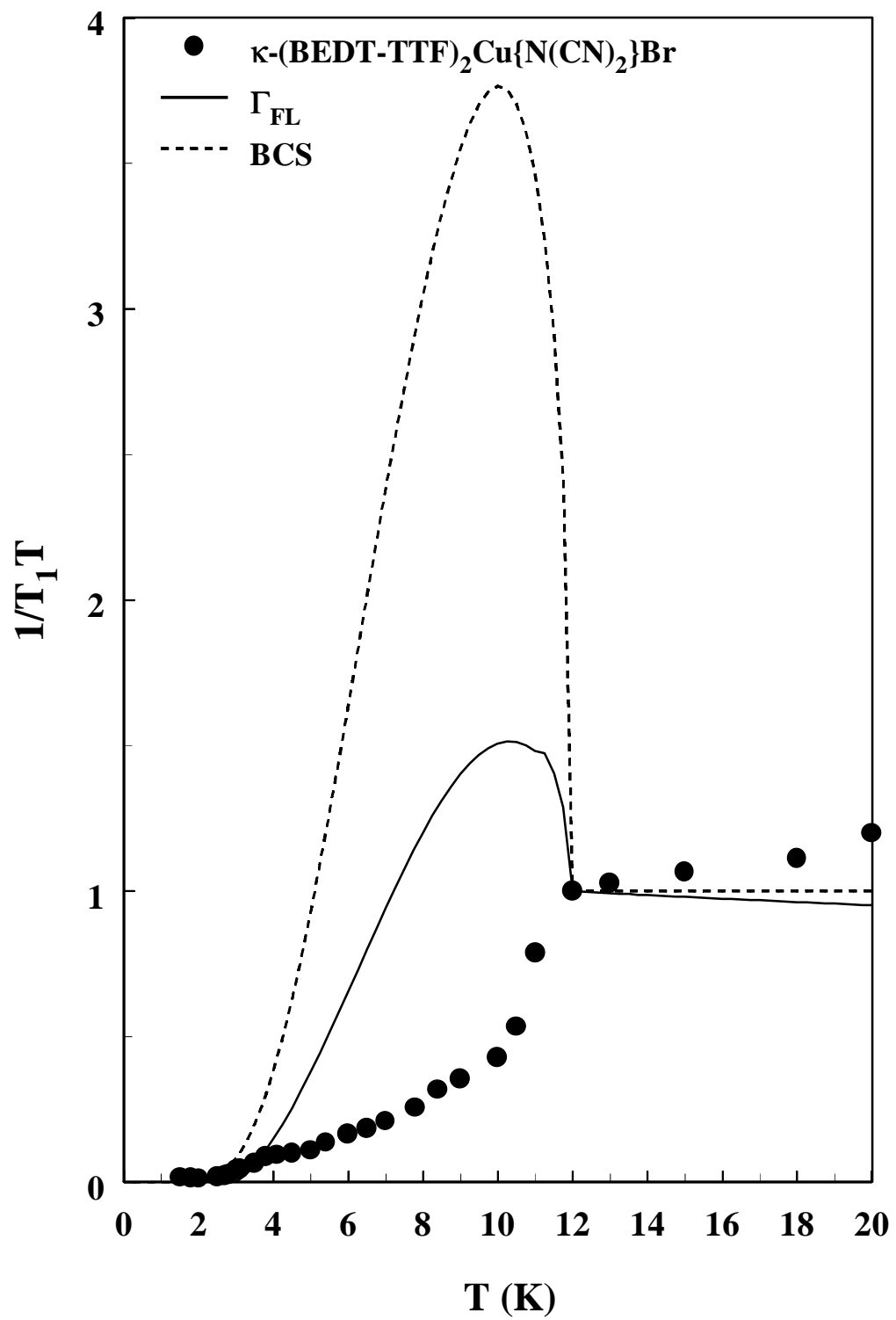


FIGURE 8

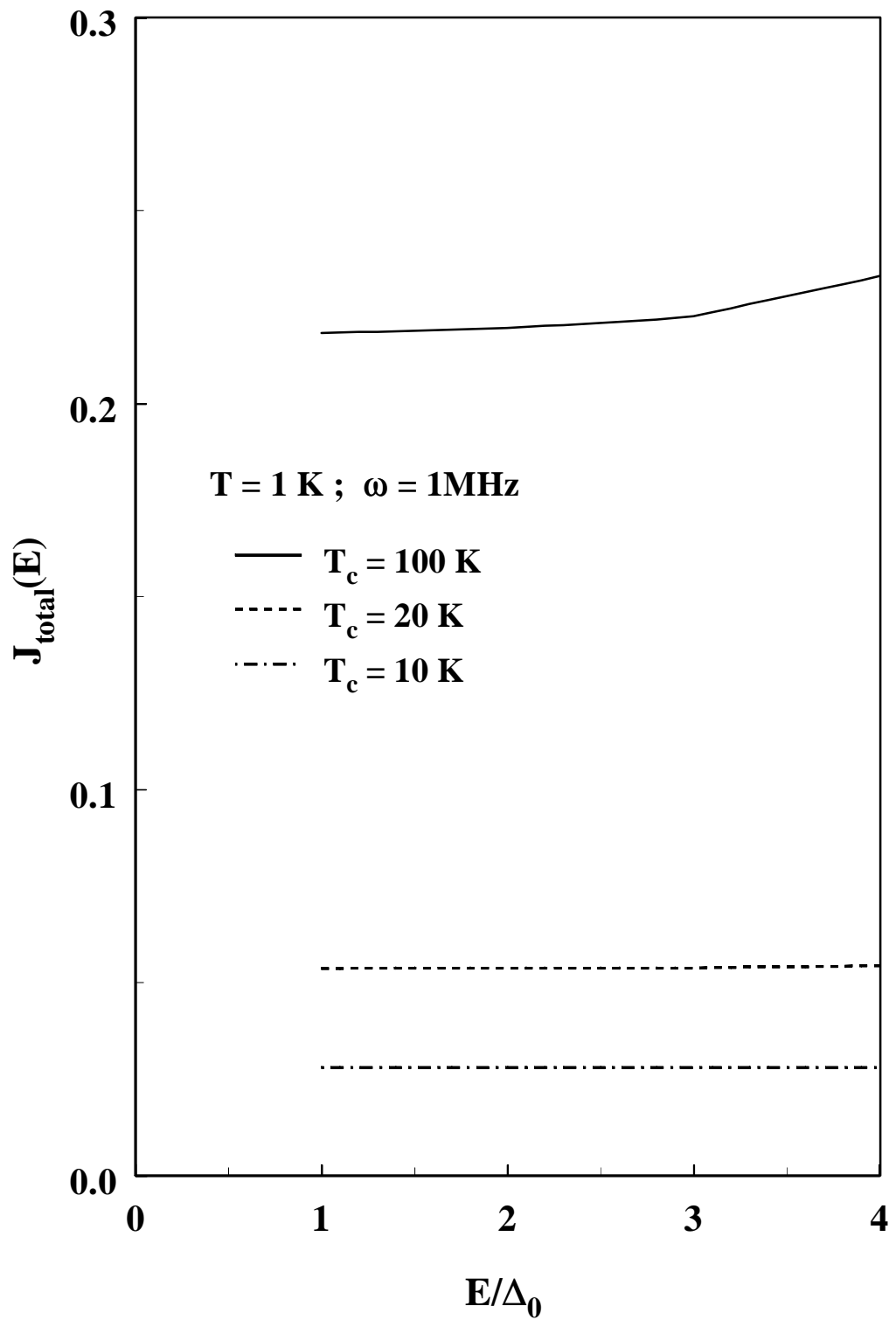


FIGURE 9